Chapter 9

Conclusions

In this thesis we have shown that MIM waveguides can be tuned over a wide range of visible and infrared frequencies by changing the device materials, dimensions, and carrier concentrations used. We have shown that by using ferroelectrics as the active material, these structures can be used as tunable color filters and using semiconducting layers, these structures can be used as electro-optic modulators.

Figure 9.1 shows the different parameters we have studied to affect the transmission spectrum through lithium niobate color filters. To the left of the waveguide, dispersion calculations plot the number of optical modes that a waveguide with a given thickness can support. Representative one- and two-dimensional mode profiles are shown within the cavity of the waveguide. The color bars to the right show that by varying the depth of the output slit into the dielectric layer, we can preferentially couple to the different photonic modes within the waveguide and change the color which is seen through the output slit. Further, by applying an electric field across these devices, we can change the refractive index of the lithium niobate and for certain combinations of slit spacing and slit depth, change the color coming through the output slit. The color bar above the waveguide shows that by varying the spacing between the input and output slits, we can couple to intensity maxima and minima of the different photonic modes that propagate through the device. Finally, initial results show that changing the dimensions of the input and output slits can increase the amount of transmitted light through the device by at least an order of magnitude. This is shown in the plot below the waveguide.

For semiconductors, namely the plasMOStor of Chapter 7, the device takes advantage of a charge accumulation effect at the Si/SiO_2 interface. Here the thickness of the device was chosen based on the dispersion calculations (top left and bottom right of Figure 9.2) so that along with the plasmonic mode, the waveguide would support exactly one photonic mode that was very near cutoff. Upon application of an electric field, the device was pushed into accumulation and the photonic mode no longer contributed significantly to the overall behavior of the device. This was confirmed

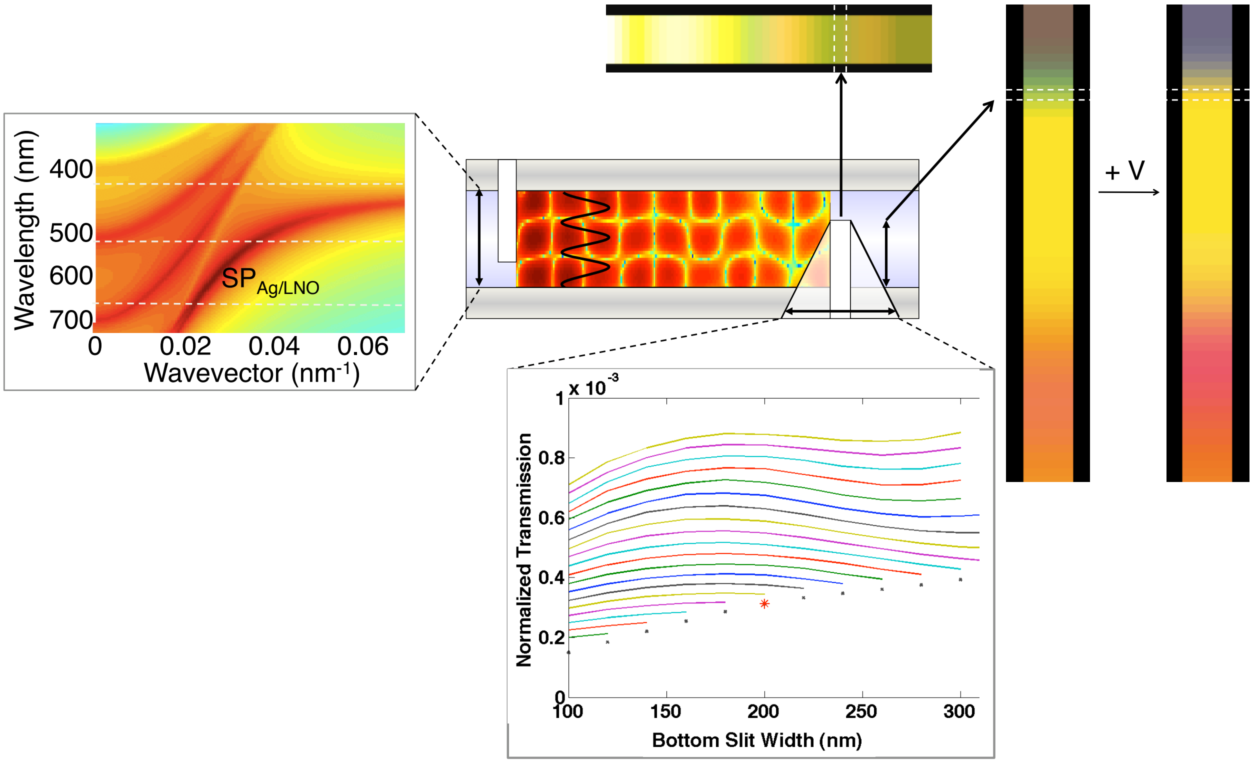

Figure 9.1. Methods for modifying the output of the MIM color filters included: varying the thickness (left); varying the depth of the output slit with and without an applied electric field (right); varying the separation between the input and output slits (top); varying the shape of the input and output slits (bottom). Representative one and two-dimension mode profiles are shown within the waveguide cavity.

using full field electromagnetic simulations which are shown in the cavity portion of the waveguide schematics (top and bottom center). Experimental measurements confirming these calculations are shown in the center of Figure 9.2, and by varying the spacing between the input and output slits, we couple to intensity maxima and minima of the optical mode(s) within the waveguide.

The above examples (as well as the TCO-based devices of Chapter 8) show the high degree of tunability associated with these structures. Although there are dozens of other parameters that could be varied with these devices, two that should be noted are: the number of input/output slits used and the strain within the films. In the future, one parameter that will be extensively studied for optimizing these devices will be using gratings to in-couple and out-couple the light. For broadband application, such as the color filters, this should prove to be a key component in improving total

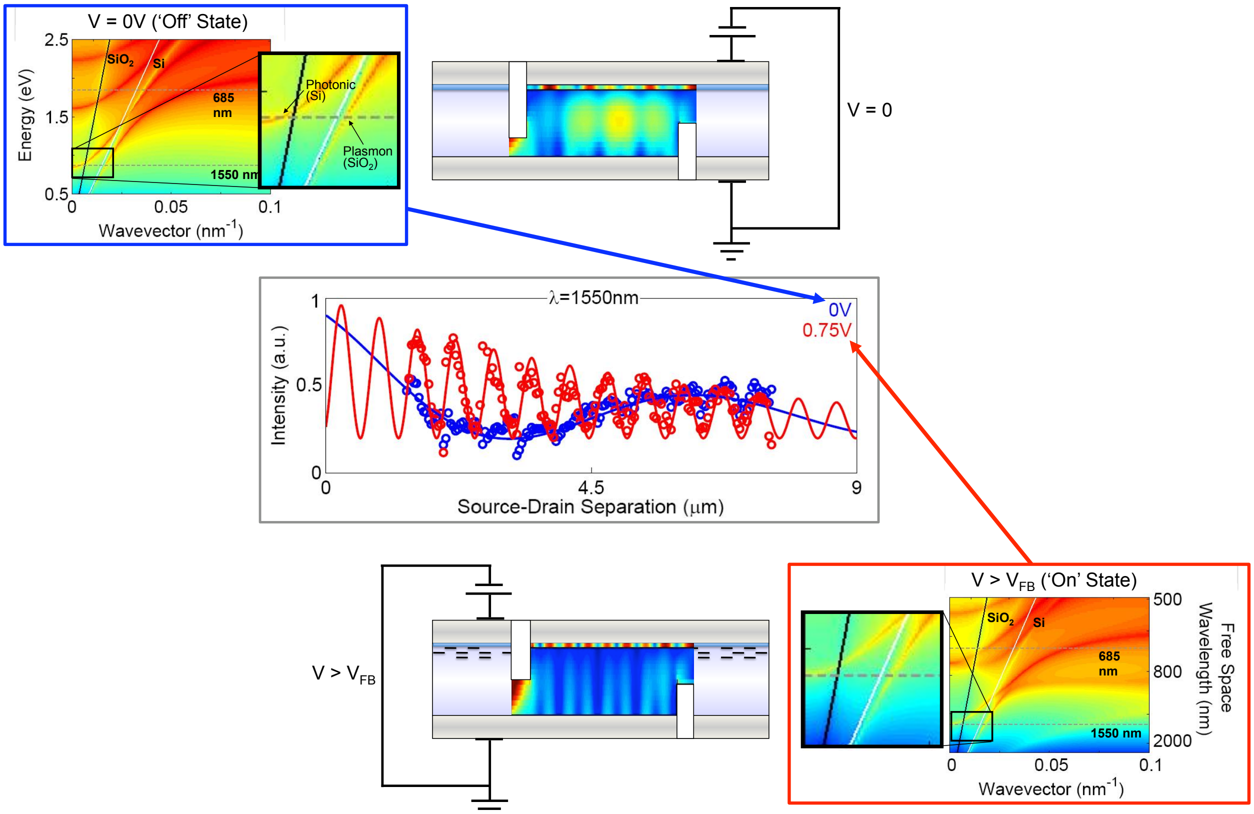

Figure 9.2. Methods for modifying the output of the MIM color filters included: varying the thickness (left); varying the depth of the output slit with and without an applied electric field (right); varying the separation between the input and output slits (top); varying the shape of the input and output slits (bottom). Representative one and two-dimension mode profiles are shown within the waveguide cavity.

power transmission and selectivity of these waveguides to individual wavelengths [85].

The issue of strain was briefly mentioned in regards to silicon in Chapter 7, Figure 7.2, and was a key component of device fabrication in Chapter 4. For the plasMostor, the strain was taken into account in calculating the effective Drude electron mass; however, the effects of strain on the refractive index were not used in any of the calculations or simulations. Similarly, for the lithium niobate color filters, Chapter 4 showed that the films must be in a state of compressive stress (but below a critical value) to form a coherent, transferred film; however, in the experiments and simulations, this was not factored into the refractive indicies used (Appendix D). A more detailed analysis of the effect of strain on the distortion of the crystal structure and resulting optical properties may provide new avenues for device applications [55].

Looking towards the future, these structures have already shown tunability across visible and infrared frequencies with both positive and negative indicies of refraction [66]. This has been done using an extremely small subset of the materials at our disposal. One future avenue of exploration that should prove extremly promising is tuning the properties of the films themselves. This has already proved useful in the simple case of varying the doping concentration of the active layer; however, calculating the dispersive properties of the materials required for a given application could open up a wide range of future applications.